ISSN 0024-9521
IJG Vol. 40, No. 2, December 2008 (115-132)

INDONESIAN JOURNAL OF GEOGRAPHY

ASSESSING THE HYPERSPECTRAL REMOTE SENSING DATA TO DIAGNOSIS CROP VARIABLES MODEL IN TROPICAL IRRIGATED WETLAND RICE

Muhamad Evri
Muhamad Sadly
sadly@webmail.bppt.go.id
Agency for The Accessment and Application of Technology, Indonesia

Arief Darmawan
Center of Technology for Natural Resources Inventory, Indonesia

ABSTRACT

Canopy spectral measurement using ground-based hyperspectral device and rice crop variables such as leaf area index (LAI), leaf dry weight (LDW) and SPAD values were done periodically during growth season with involving three rice cultivars (Pandanwangi, Ciherang and IR Jumbo) and four nitrogen application levels (N0, N80, N92 and N103 kg/ha). The study is directed to explore all possible waveband combinations tested in reflectance of vegetation indices (VIs) and to develop a predictive model of relation between hyperspectral-based vegetation indices with rice crop variables.

Analysis of all possible two-pair waveband combinations used in VIs was investigated with 6,786 combinations to gain optimal waveband attributed to crop variables. To develop efficient and accurate model, various multivariate regression models were examined with ten-fold cross validations. Accuracy validation of predicted model was performed using reflectance and FDR, NDVI, RVI, RDVI and SAVI data. Validation of predictive model using FDR implied better accuracy to estimate LAI using whole season data (R^2=0.856). Meanwhile, the model using SAVI denoted highest values (R^2=0.852) for predicting LAI. While the validation of predictive model using RVI implied the highest values (R^2=0.797) for predicting LDW. Moreover, the test of predictive model using SAVI indicated the highest value (R^2=0.658) for predicting SPAD values. According to overall validation using VIs, it seems that RVI has the best accuracy to validate the predictive model of LAI than those of LDW or SPAD values. Meanwhile, the most significant of R^2 to validate the predictive model was obtained on FDR data with R^2=0.859 for LAI.

Keywords: visible, near-infrared, hyperspectral, vegetation indices, crop variable, predictive model.

INTRODUCTION

Asian countries are dependent on rice as major staple food for Asian countries. The importance of rice endorses countries to sustain the rice availability with many ways, such as applying technologies to observe the current status of rice. Remote sensing techniques have high potential to provide quantitative, instantaneous, and nondestructive information on rice over a large areas.

Estimation ability for rice biophysical parameters and its productions in the fields from remote sensing images is not only fundamental in agriculture application precision, but it can be very useful for food provisions management. Remote sensing technique, well known, has an advantage in providing temporaly information with fair accuracy and precision on the current status of interested targets, however the spectral nature of crop vegetation and the relationships between image spectral characteristics and crop variable should be well defined and clarified in laboratory and in the field as well, before practical agricultural applications are performed [*Yang* and *Su*, 1997]. In past years, varied spectral indices have been developed from spectral transformation of several wavebands to improve the radiometric measurement of crop vegetation and to monitor and evaluate vegetation development [*Anderson* and *Hanson*, 1992]. The ratio-based spectral indices such as NDVI [*Gilabert et al.*, 1996] and soil adjusted vegetation indices (SAVI) [*Huete*, 1988] were designed to minimize interferences by internal geometry noise caused mostly by plant structure and population architecture, and external radiation influences due mainly to solar angle and atmospheric properties [*Elvidge* and *Chen*, 1995].

The normalized transformations generally incorporate the functions of red and near-infrared bands of a vegetation spectrum and result in a nonlinear measure of biophysical parameters. It is well known that reflectance in red light is negatively correlated with chlorophyll concentration while reflectance in the near-infrared is positively correlated with leaf area [*Tucker*, 1979; *Tucker et al.*, 1979]. In addition, spectral indices have been widely used in many agricultural applications and combined with various growth models for vegetation growth and activity comparison in field, regional, and global scales [*Elvidge* and *Chen*, 1995].

In addition to spectral indices, combining spectral reflectance from two or more characteristics wavebands into single numbers may improve sensitivity to plant vegetation relative to using individual bands [*Wanjura* and *Hatfield*, 1987]. Many studies on this subject have demonstrated relationships between spectral characteristics and vegetation attributes through regression analysis where multiple regression models provide flexibility in choosing discrete narrows bands and give better information from spectral data [*Shibayama* and *Akiyama*, 1991]. However,

the band combinations which provided optimal information are influenced by growth status of the crop, whose characteristics differ among phenological stages and are affected by environmental conditions and cultural practices [*Thenkabail et al.*, 2001]. The collinearity between wavebands may also result in *overfitting*, using more spectral bands than are necessary [*Thenkabail et al.*, 2001]. It is therefore interesting to examine the optimal waveband combinations from hyperspectral reflectance data for a possibility of improving the relationships by using growth parameters in specific crops.

THE METHOD

Experiments for this research was carried out at tropical irrigated wetland rice area at Karawang district, West Java, Indonesia (6°14'50.9"S and 107°20'29.4" E). This area is a lowland and flat area, near to the north coast of Java Island. Paddy field is technically innundated through irrigation network supplied from Jatiluhur reservoir.

Canopy spectral irradiance in the range of 350 to 1050 nm was measured by using a high spectral resolutions (1 nm intervals) portable spectroradiometer (MS-720) [*EKO Instruments*, 2004]. The device was equipped with an integrated LCD, a small-sized grating spectrometer, diode array, and internal memory. The entire measurements were performed on cloudless or near cloudless days, started on 9 am until 12 am local standard time. Measurements were undertaken periodically (approximately every week) at each plot, pointed downward from 1 m above the canopy, with aperture angle of FOV 45°. In addition, measurements were executed consecutively three times per plot to reduce the possible effect of changing sky conditions. A spectral on (Labsphere, Inc., Sutton, NH, USA) reference panel was used to optimize the EKO instrument prior to taking canopy reflectance measurements at each plot.

Plant sampling was undertaken coincided with spectral measurement. Samplings were purposed to collect crop variables information such as leaf area index (LAI), leaf dry weight (LDW) and SPAD values which are commonly used as a growth status indicators. Ten leaves of representative hills were randomly measured using Minolta SPAD-502 chlorophyll meter for obtaining the mean value of SPAD.

Data processing

Spectral domain which displayed low signal-to-noise ratio in both ends of the spectrum (325-397; 983-1050 nm) was first omitted and then spectral wavebands were averaged into 5 nm wavelength to reduce the noise and amount of data for analysis, resulting in a total of 117 spectral bands between 400 nm and 980 nm. A first derivative reflectance (FDR) spectra was calculated corresponding to

method introduced by [*Dawson* and *Curran*,1998] and smoothed using Savitzky-Golay method [*Savitzky* and *Golay*,1964]. A first difference transformation of the reflectance spectrum (FDR), which calculates the slope values from the reflectance, was derived from the following equation [*Dawson* and *Curran*,1998]:

$$FDR_{\lambda(i)} = \frac{(R_{\lambda(j+1)} - R_{\lambda(j)})}{\Delta_\lambda} \quad \ldots\ldots (1)$$

where FDR is the first derivative reflectance at a wavelength *i* midpoint between wavebands *j* and *j* + *1*. $R_{\lambda(j)}$ is the reflectance at waveband j, $R_{\lambda(j-1)}$ is the reflectance at waveband *j* + *1*, and Δ_λ is the difference in wavelengths between *j* and *j* + *1*. Averaged 5 nm wavelength intervals were used to define the intervals between channels *j* and *j* + *1*.

The analysis was carried out by three growing seasons of paddy crop respectively, namely (1) pooled whole-season data (DAT 19 – 80, n = 132) and focused on (2) before-heading (DAT <= 47, n = 72) and (3) after-heading data (DAT > 47, n = 60). These data sets were first randomly divided into calibration (2/3) and validation data (1/3) sets. Afterward, calibration model was developed using calibration data set. The end step of all, the model was validated by comparing between predicted values (from the model) and measured value (from laboratory measurement) in the validation data set. In the first analysis, the linear regression analyses of LAI, LDW and SPAD with all of corresponding reflectance and FDR spectra data throughout the wavelength ranged from 400 to 980 nm in the calibration data set were performed. Afterward, the next step is to determine reflectance and FDR in the calibration data set which having the greatest R^2 values with crop variables. In the second analysis, four selected vegetation indices (VIs), such as (1) RVI, (2) NDVI, (3) RDVI and (4) SAVI were calculated for all available waveband combinations. The VIs were calculated using following equations as is represented in Table 1. The narrow bands are computed as λ_1 and λ_2 derived from selected-waveband in reflectance or FDR spectra.

Table 1. Vegetation Indices Formulae used in This Study.

Index name	Formulae
Normalized Difference Vegetation Index (NDVI)	$\frac{(\lambda_1 - \lambda_2)}{(\lambda_1 + \lambda_2)}$
Renormalized Difference Vegetation Index (RDVI)	$\frac{(\lambda_1 - \lambda_2)}{\sqrt{(\lambda_1 + \lambda_2)}}$
Ratio Vegetation Index (RVI)	$\frac{\lambda_1}{\lambda_2}$
Soil Adjusted Vegetation Index (SAVI)	$\frac{(\lambda_1 - \lambda_2)(1 + L)}{\sqrt{(\lambda_1 + \lambda_2 + L)}}$

RESULT AND DISCUSSIONS

(a) Overview of the spectral reflectance data

Average reflectance data at each growth stage of the three rice cultivars and four N application levels is presented in Fig. 1. Spectral variations among curves are mainly due to differences in crop growth stages. Lowest reflectance values in near infrared wavelengths (700 – 1000 nm) were observed for early developmental stage, where biomass was still not dense and spectral reflectance was mainly influenced by soil and water background. Maximum reflectance in the NIR was observed at the heading stage, which was coincident with maximum values of green Leaf Area Index.

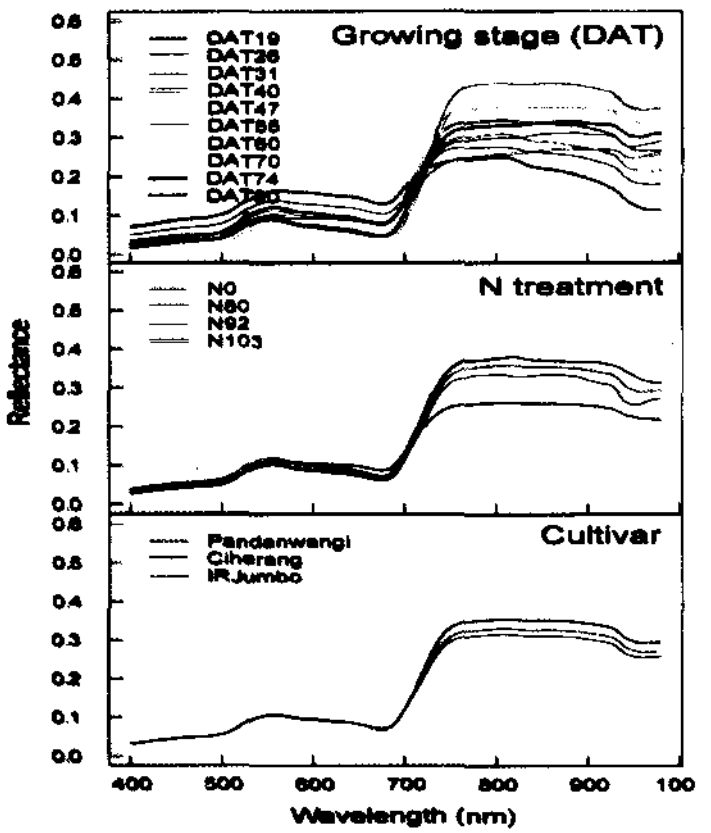

Figure 1. Average reflectance spectrum of rice canopy at different (a) growing stage (*n = 12 for each stage*), (b) N level (*n = 33 for each N treatment*) and (c) cultivar (*n = 44 for each cultivar*)

The increase of reflectances at NIR waveband was related to increases of crop biomass, LAI and canopy water, while the reduction in reflectance at red waveband potentially resulted from the increase of leaf chlorophyll and N. It consequently shows low reflectance of solar radiation in red wavelengths and high scattering of solar radiation in NIR. At heading until maturity stages, reflectance in visible (400–700 nm) and NIR (700-1000 nm) regions increased and decreased, respectively. This case is mainly caused by the increase of number of senescent leaves.

The reflectance at NIR of Pandanwangi cultivar is higher than both cultivars, i.e IR Jumbo and Ciherang cultivar. This point can be explained by physical appearance, where Pandanwangi cultivar had bigger and wider sizes of leaf blade than the others. Likewise, IR Jumbo cultivar had bigger and had wider sizes of leaf blade than that of Ciherang cultivar. In the visible waveband region, the differences of reflectance among cultivars were small. The changes of the spectral reflectance pattern in rice canopy at every stage are shown in Figure 1a. The reflectance of early growth stage shows a peak at green spectrum within visible waveband and relatively high value at 559 nm and 807 nm within infrared wavebands. Spectral reflectance in visible waveband domain changed from high to low with increasing of LAI, however, spectral reflectance of infrared waveband was increased with increasing of LAI. The reflectivity of visible band remained less than 0.1, but near infrared band ranged from 0.1 to 0.4 throughout growing season.

Furthermore, on Fig. 1b shows that application of N rates of 103 kg/ha increased reflectance at near-infrared waveband (>760 nm) higher than that of N rates of 92.80 and 0 kg/ha, respectively. Likewise, application of N rates of 92 kg/ha increased reflectance at near-infrared waveband higher than that of N rates of 80 and 0 kg/ha, respectively. Near infrared waveband of 800 nm, reflectance of three cultivars is significantly different, as was already mentioned above. In general, the reflectance of each N rate indicated similar trend, where they decreased at red waveband, and increased at NIR waveband.

(b) Correlation of crop variables with canopy reflectance and FDR

The relation as is indicated by coefficient of determination (R^2) calculated by regression analysis among reflectance and FDR with crop variables (LAI, LDW, and SPAD) represented various results (Fig. 2). LAI, LDW and SPAD value represented positive correlation with both reflectance and FDR, at whole season, before heading and after heading, respectively. Among those relations, LAI and FDR at whole season hold the most significant relation at 735 nm (R^2 = 0.897), than that of before and after heading. However, overall relations generally pointed out the significant correlations. In addition, the relation of LAI and LDW with reflectance at whole season implied significant values (R^2 = 0.849) at the same

waveband (890 nm) in Figure 2. Likewise, the relation of LAI and LDW with reflectance at after heading indicated significant values (R^2 = 0.891 for LAI and 0.743 for LDW) at the same waveband (775 nm). Meanwhile the correlation LAI, LDW and SPAD value with FDR at after heading represented significant correlation (R^2 = 0.891 for LAI, 0.845 for LDW and 0.752 for SPAD) with close waveband (730 nm for LAI, 740 nm for LDW and 720 nm for SPAD value, respectively).

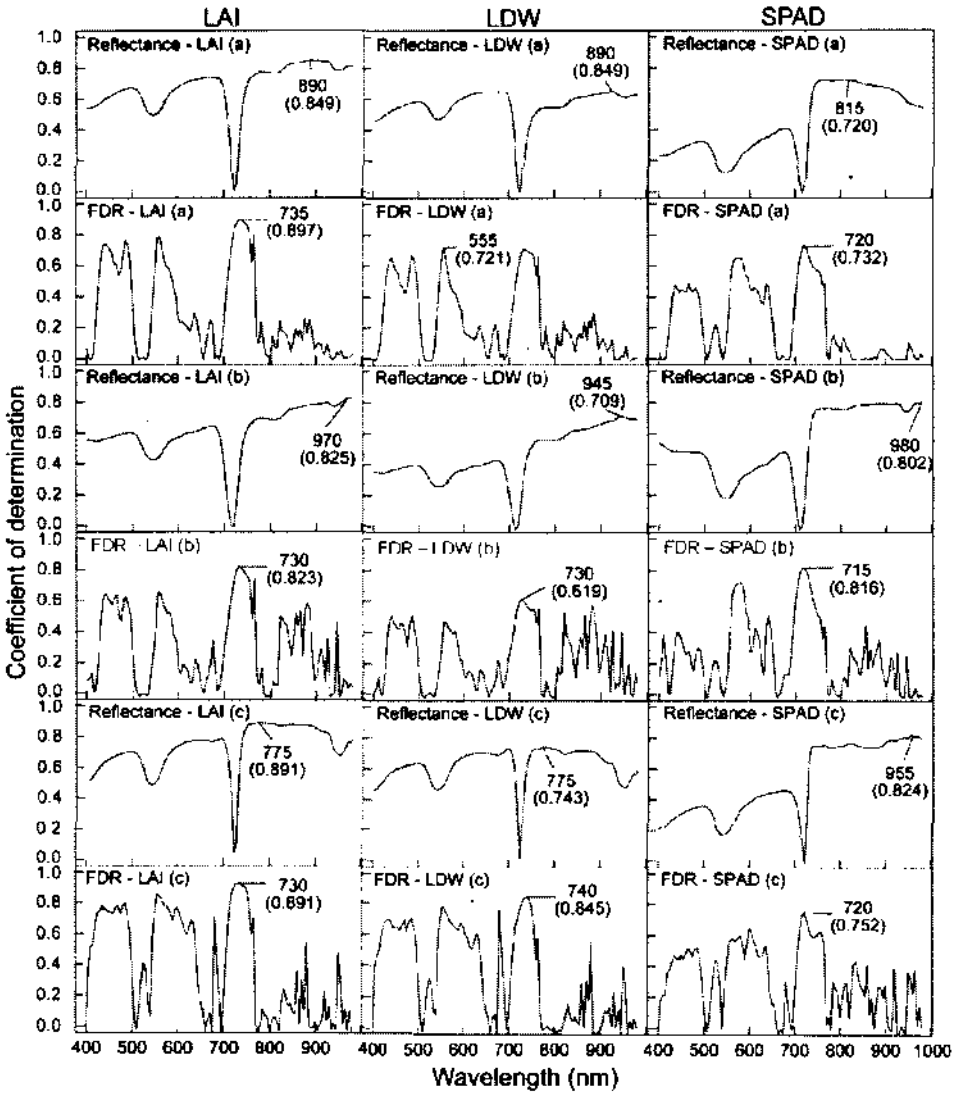

Figure 2. The relation among reflectance and FDR with LAI, LDW and SPAD at whole- (a), before- (b) and after-heading (c) stages. Typical wavebands are highlighted in the figure, indicated by greatest R^2 (in parenthesis)

(c) Best paired-waveband for vegetation indices to predict crop variables

Analysis of all possible two-pair combinations of waveband ($Waveband_2 > Waveband_1$) used in VIs was investigated with 6,786 combinations to gain optimal waveband attributed to crop variables. The linier regression was performed in order to determine the correlation coefficient (R^2). The results of R^2 were plotted in a matrix plot and the plot revealed a characteristic pattern with a number of "hot spots" with relatively high correlate on coefficients (Fig. 3 and Fig. 4). These spots were selected by choosing the wavebands combinations that showed an R^2 between 70% and 100% of the overall best index. A number of "hot spots" with high correlation coefficient were revealed in a linier regression analysis of the individual crop variables toward VIs calculated according to equations in Table 1 for all possible two-pair combinations of the reflectance measured at the 117 wavebands. Best-3 of "hot spot" resulted from analysis of all possible of waveband combination using both $waveband_2$ and $waveband_1$ with crop variables were revealed in Table 4.

The typical selected wavebands through all combinations bands that used in VIs varied across crop variables and growing stage. The vegetation indices (VIs) were calculated for all available waveband combinations between 400 nm and 980 nm to define the best paired combination of wavebands attributed to crop variables. Several paired wavebands with high R^2 values were found in LAI ($R^2 > 0.80$, green area in Fig.3a), LDW ($R^2 > 0.60$, light-red area in Fig.3b) and SPAD values ($R^2 > 0.50$, orange area in Figure 3c). The significant relations were represented in the domain of shorter waveband in red edge (700 – 760 nm) to LAI and LDW. Meanwhile, the second highest R^2 values for SPAD values attained when combined with narrow bands in the blue (400 – 495 nm) and mixing green and red (600 – 700 nm) regions, in particular for RDVI and SAVI. The highest R^2 values for LAI were obtained by waveband combinations that ranged from blue, green and red region (400 nm to 740 nm), in particular for RVI, RDVI and SAVI. Whereas for NDVI the highest R^2 values for LAI were found waveband combinations, ranged from green to red region (500 nm to 730 nm).

Fig. 4 demonstrates relations for all waveband combinations used in VIs toward (a) LAI, (b) LDW, and (c) SPAD, respectively before and after-heading. All possibilities of 6,786 waveband combinations were investigated to achieve best band-paired. Several paired wavebands with high R^2 values before and after heading were found in LAI ($R^2 > 0.80$, light green area in Figure 4a). Meanwhile, paired-wavebands with high R^2 values before and after heading in LDW shows that domain with $R^2 > 0.60$ represented by red area before heading, whereas domain with $R^2 > 0.80$ after heading represented by RVI, NDVI and RDVI (yellow to green area) in Figure 4b. Paired-wavebands with high R^2 values before and after heading for SPAD values indicate that region with $R^2 > 0.80$ (bright area) is represented by RDVI and SAVI before heading, whereas for after heading, region with $R^2 > 0.70$

is shown by orange area. The region with $R^2 > 0.60$ after heading was represented by RVI and NDVI (red area) in Figure 4c. In general, the numbers of optimal paired-wavebands used in VIs for LAI exceed the number of optimal paired-wavebands used for LDW and SPAD.

The wavebands in red and NIR ranged from 635 nm to 840 nm were selected in the best-3 of R^2 values derived from waveband combinations for LAI before heading and ranged from 715 nm to 735 nm after heading (Table 4). The highest R^2 (0.923) is represented by pairing wavebands of 720nm and 725 nm for after heading. From the Table 4 also, it looks that Band 1 and Band 2 are dominated by NIR wavebands (820 nm to 840) for whole season and for NDVI, RDVI and SAVI, while for RVI, Band 1 and Band 2 are dominated by red wavebands (715 nm and 730 nm for Band 1 and 515 nm to 610 nm for Band 2). In the case of before heading stage, there are variations of Band 1 and Band 2 that involved in band combinations, where for RVI and NDVI, red waveband used in Band 1 (685 nm to 695 nm) and Band 2 (715 nm to 725 nm). Whereas for RDVI and SAVI, NIR waveband dominantly used in Band 1 (840 nm to 850 nm) and red waveband dominantly used in Band 2 (745 nm). In the case of after heading stage, involved band combinations in all VIs are represented by red wavebands for Band 1 (715 nm to 735 nm) and Band 2 (700 nm to 720 nm).

The best-3 of R^2 derived from waveband combinations used in VIs for LDW ranged from 750 nm to 840 nm, 520 nm to 740 nm and 690 nm to 905 nm before heading, after heading and whole season, respectively (Table 4). Generally, from the same table it seems that Band 1 dominated by NIR wavebands (825 nm to 905 nm) and Band 2 dominated by red wavebands (670 nm to 755 nm) for whole season and before heading and for all VIs, while for after heading, Band 1 and Band 2 are represented by red that ranged 730 nm to 735 nm and 590 nm to 740 nm, respectively. The highest R^2 are generally obtained from involving wave band combinations in red region for LDW and for VIs after heading, while during before heading and whole season, the highest R^2 represented by combinations of Band 1 and Band 2 in NIR (825 nm to 840 nm) and red region (670 nm to 755 nm), respectively.

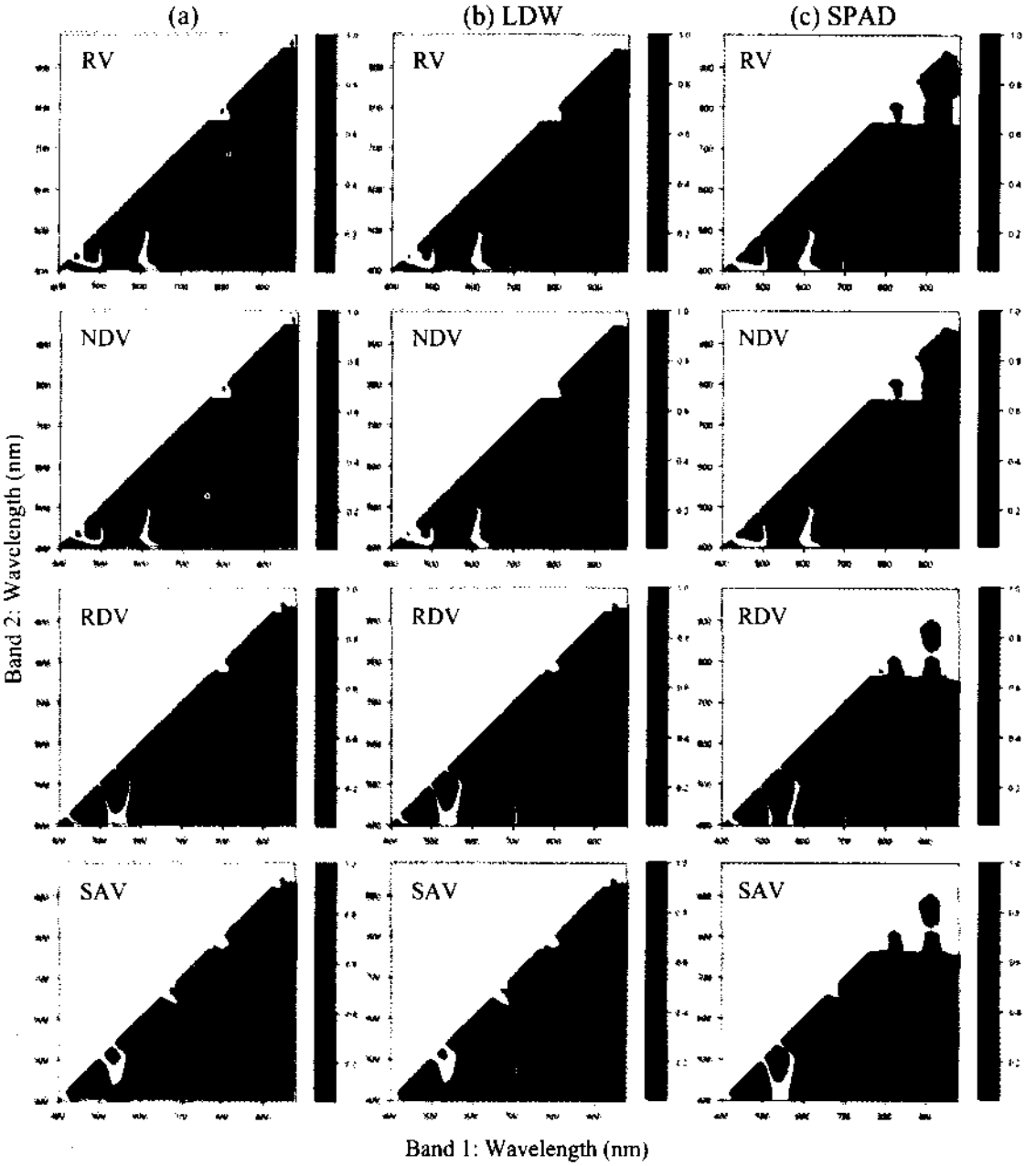

Figure 3. Coefficients of determination (R^2) of the relation for all wavelength combinations used for linear regression analysis of the four VIs against (a) LAI, (b) LDW, and (c) SPAD, respectively, in the calibration data for whole-season (n = 88). A total number of 6,786 combinations were investigated

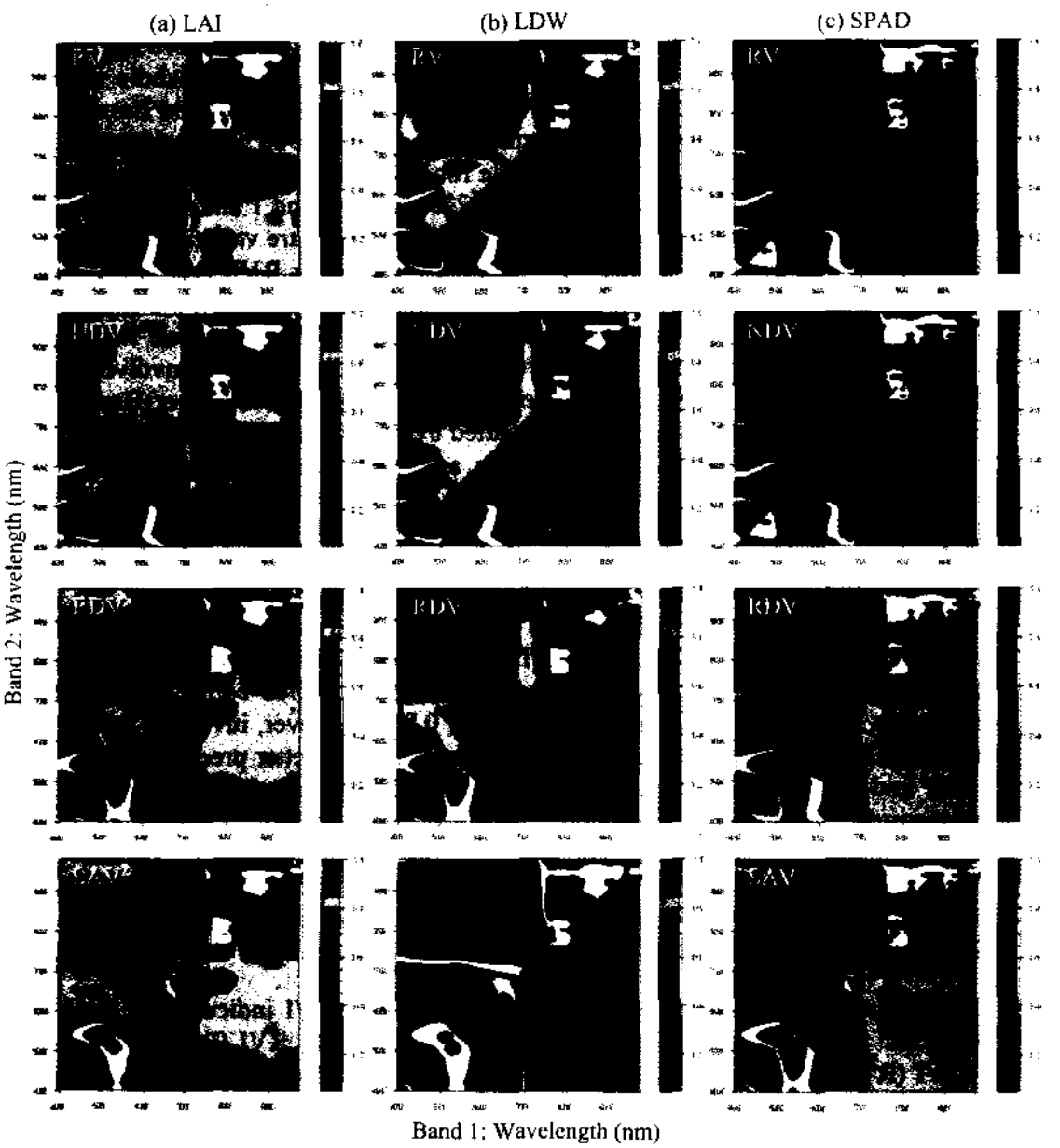

Figure 4. Coefficients of determination (R^2) of the relation for all waveband combinations used in linear regression analysis of the four VIs against (a) LAI, (b) LDW, and (c) SPAD, respectively, in the calibration data for before- (bottom-right, n = 48) and after-heading (top-left, n = 40). A total number of 6,786 combinations were investigated

As for the relations VIs with SPAD, the best-3 of R^2 was derived from waveband combinations for SPAD ranged from 405 nm to 895 nm, 410 nm to 955 nm and 525 nm to 720 nm for before heading, after heading and whole season, respectively (Table 4). From the Table 4 also, it looks that Band 1 and Band 2 are dominated by green wavebands (535 nm to 545 nm and 525 nm to 530 nm) for whole season and for RVI and NDVI, while for RDVI and SAVI, Band 1 and Band 2 are dominated by red region (715 nm and 720 nm for Band 1 and 705 nm to 715 nm for Band 2). In the case of before heading stage, there are variations of Band 1 and Band 2 that involved in band combinations, where for RVI, green waveband used in Band 1 (525 nm to 535 nm) and red waveband used in Band 2 (715 nm). Whereas for NDVI, NIR waveband used in Band 1 (820 nm) and blue waveband used in Band 2 (425 nm to 440 nm). In the case of RDVI and SAVI, involved band combinations in both VIS indicated the variation of wavebands, either Band 1 or Band 2, but in general it seems still dominated by red domain for Band 1 and green region for Band 2, respectively. Meanwhile, as for after heading stage, for Band 1 is dominated by NIR wavebands (955 nm) and Band 2 is dominated by red waveband (715 nm to 725 nm).

(d) Validation data set for prediction of rice crop variables

Comparisons of MLR models (measured and predicted values) using reflectance and FDR, NDVI, RVI, RDVI and SAVI (Fig. 5) show significant correlations ($R^2 > 0.57$). Model using FDR for LAI implied better accuracy for predicting LAI using whole season data ($R^2 = 0.86$), however, inversely for LDW and SPAD values, model using reflectance data indicated better precision to predict LDW and SPAD values, as are represented by their R^2, namely 0.651 and 0.707, respectively. Meanwhile, the model using SAVI denoted the highest values ($R^2 = 0.852$), then followed by RDVI ($R^2 = 0.845$), RVI ($R^2 = 0.816$) and NDVI ($R^2 = 0.785$) for predicting LAI.While the validation of predictive model using RVI implied the highest values ($R^2 = 0.797$), then followed by SAVI ($R^2 = 0.756$), RDVI ($R^2 = 0.754$) and NDVI ($R^2 = 0.731$) for predicting LDW.

Moreover, the test of predictive model using SAVI indicated the highest value ($R^2 = 0.658$), then followed by RDVI ($R^2 = 0.644$), RVI ($R^2 = 0.566$) and NDVI ($R^2 = 0.565$) for predicting SPAD values. According to overall validation using VIs, it seems RVI has the best accuracy to validate the predictive model of LAI than that of LDW or SPAD values. Meanwhile, the most significant of R^2 to validate the predictive model is using FDR data with $R^2 = 0.859$ for LAI.

Table 2. Best 3 of two-band combinations for the relationships of RVI, NDVI, RDVI and SAVI

Crop variable	Data season	Index	RVI			NDVI			RDVI			SAVI		
			Band 1	Band2	R^2	Band 1	Band2	R^2	Band 1	Band2	R^2	Band 1	Band2	R^2
LAI	Whole-season	1	730	520	0.888	825	720	0.883	835	720	0.908	840	715	0.906
	(n=88)	2	730	515	0.888	820	720	0.882	840	715	0.908	835	715	0.906
		3	715	610	0.888	825	715	0.882	835	715	0.907	835	720	0.906
	Before-heading	1	695	635	0.910	685	670	0.908	845	745	0.894	845	745	0.893
	(n=48)	2	985	670	0.910	690	655	0.904	840	745	0.893	840	745	0.892
		3	690	655	0.908	685	675	0.901	845	745	0.893	850	745	0.891
	After-heading	1	725	720	0.904	725	720	0.904	725	720	0.921	725	720	0.923
	(n=40)	2	725	715	0.904	725	715	0.903	730	720	0.921	730	720	0.922
		3	715	700	0.901	730	715	0.902	735	715	0.920	735	715	0.921
LDW	Whole-season	1	690	675	0.768	825	725	0.767	840	725	0.763	835	725	0.765
	(n=88)	2	690	670	0.767	830	725	0.767	835	725	0.763	840	725	0.765
		3	905	720	0.767	825	730	0.766	835	730	0.762	835	730	0.765
	Before-heading	1	690	675	0.768	835	750	0.730	835	755	0.759	835	755	0.757
	(n=48)	2	690	670	0.767	840	750	0.725	840	750	0.755	840	750	0.755
		3	905	720	0.767	825	755	0.719	835	750	0.753	835	750	0.753
	After-heading	1	740	730	0.854	590	520	0.852	740	730	0.857	740	730	0.857
	(n=40)	2	735	730	0.852	740	735	0.851	740	735	0.857	740	735	0.857
		3	745	730	0.852	740	730	0.850	735	730	0.855	735	730	0.856
SPAD	Whole-season	1	540	530	0.668	540	530	0.667	715	710	0.705	715	710	0.711
	(n=88)	2	545	525	0.665	545	525	0.666	720	710	0.704	720	710	0.710
		3	535	530	0.663	535	530	0.664	720	715	0.700	720	705	0.707
	Before-heading	1	715	525	0.746	820	440	797	830	405	0.848	730	520	0.845
	(n=48)	2	715	530	0.745	820	425	0.797	730	515	0.848	730	525	0.848
		3	715	535	0.742	820	435	0.9797	730	520	0.847	895	405	0.848
	After-heading	1	955	725	0.700	955	725	0.718	955	420	0.797	955	410	0.812
	(n=40)	2	955	720	0.695	955	720	0.714	955	415	0.797	955	415	0.812
		3	940	725	0.688	955	715	0.708	955	410	0.797	955	420	0.811

The selection of wavebands has been undertaken in connection with known canopy characteristics. The approach in present experiment was more extensive, where all available waveband combinations were tested in NDVI, RVI, RDVI and SAVI to be attributed to crop variables. The spectral properties of the canopy were not used directly to analysis crop variables, but tested in VIs as showed by a matrix plot "hot spot", which is a sort of two-dimensional corellogram (Fig. 3 and Fig. 4). The advantage the matrix plots is that they give a quick overview of thousands waveband combinations and make it possible to detect interesting wavebands for further analysis.The band combinations were often paired so that both bands were closely spaced in the steep linear shift between Red and NIR. This index proved in fact to give the best description of the three crop variables (LAI, LDW and SPAD values), and all expressing quantity per unit soil surface or canopy area. The use of VIs implies that closely space narrow bands indicate the slope of the reflectance, which often is referred to as a derivative vegetation index [*Elvidge* and *Chen*, 1995].

Generally, even if four VIs yielded high coefficient of determination (R^2) against crop variables, however the mean R^2 calculated from the first 30 band combinations were higher for RDVI and SAVI than that of RVI and NDVI after heading for LAI and LDW, and before heading for SPAD (Fig. 4). Therefore, RDVI and SAVI may be better indices for diagnosing and predicting crop variables that relating to particularly biomass in dense canopies. The performance of reflectance was directly affected by divergent treatments (Fig. 1). In general view, it looked that the pattern of change of reflectance was similar for all the treatments. Increasing of plant density, nitrogen level and growth stage cause increasing of greenness, reflecting a combination of biomass and chlorophyll density.

The variation of R^2 values denotes that narrow band combinations tested in VIs respond differently toward biomass. The study has shown that crop variables information is not only contained in the red absorption and NIR wavelengths. Most narrow bands tested in RVI, NDVI, RDVI and SAVI, which yielded the highest correlation against crop variables, were located in the red edge region (Fig. 3 and Fig. 4).

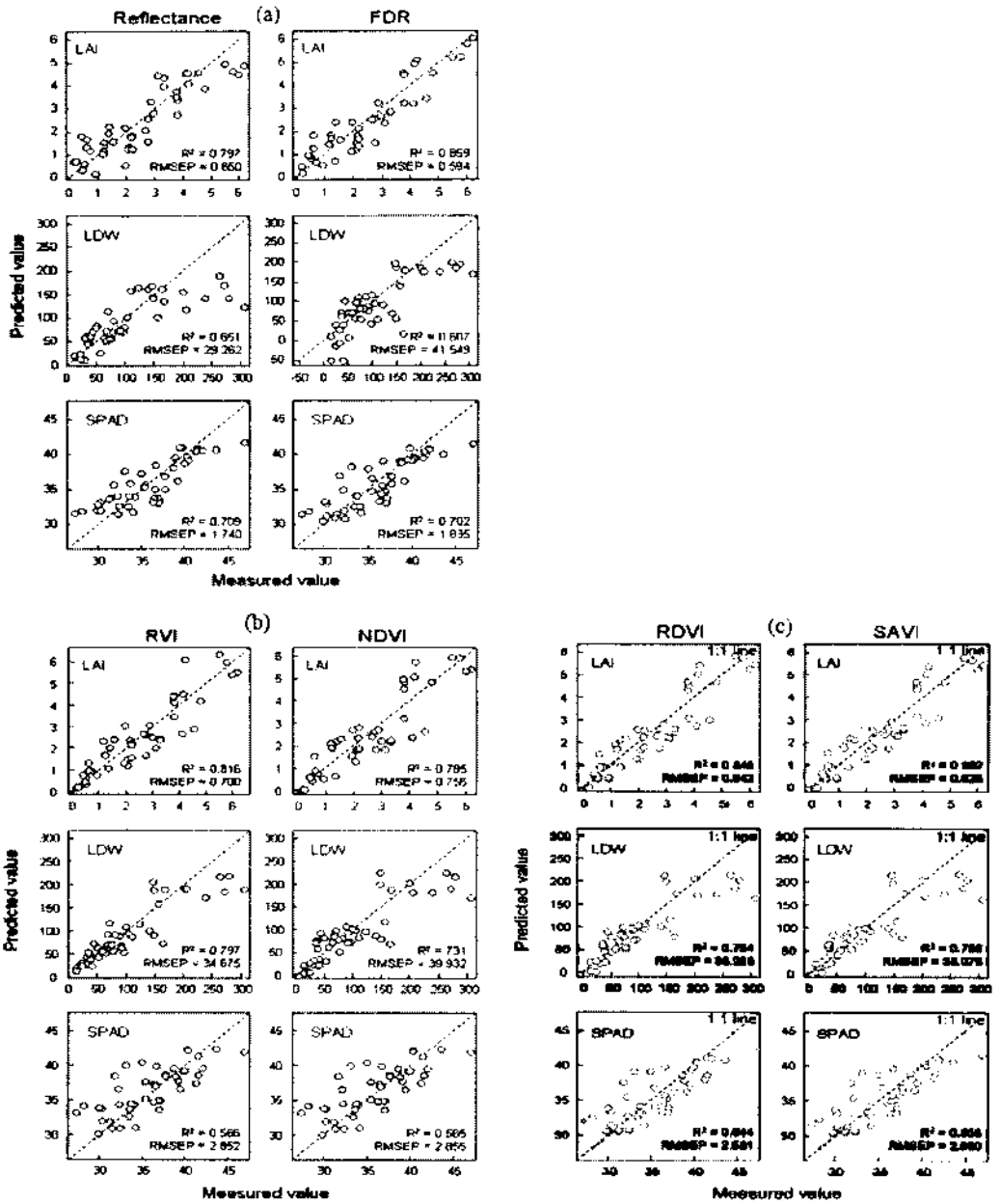

Figure 5. Validation of laboratory measurement of crop variables (LAI, LDW and SPAD) with reflectance and FDR (a), RVI and NDVI (b), and RDVI and SAVI (c) with their predictive values from MLR regression analysis using reflectance and FDR data (a) and Vis data (b and c) during growth season

Furthermore, the red edge position influenced a high correlation of determination (R^2) with crop variables. The red edge exhibits a region of transition from strong chlorophyll absorption to near infrared reflectance. High correlations in this study were largely obtained by combining narrow bands from the shorter wavelengths of the red edge portion of the electromagnetic spectrum (700-750 nm) and the longer wavebands of the red edge (750-800 nm). The shorter wavebands of the red edge portion are sensitive to changes in chlorophyll content [*Filella* and *Penuelas*, 1994; *Lichtenthaler et al.*, 1996]. At longer wavebands of the red edge domain, multiple scattering from leaf layers results in higher reflectance (*Kumar et al.*, 2001). Chlorophyll concentration and some extent other pigment in the leaves play a major role in coloring the canopy during vegetative growth stages. This agrees with the fact that visible wavebands seem to be important for indices related to crop variables expressing a concentration of either chlorophyll or leaf nitrogen. Problems due to saturation have previously been reported for NDVI and SAVI, using red and NIR, while it was less pronounced for green NDVI [*Daughtry et al.*, 2000].

CONCLUSION

Selection of the optimal waveband combinations tested in VIs improved the relationships to crop variables. Validation of predictive model using FDR implied better accuracy to estimate LAI using whole season data (R^2 = 0.859), however, inversely for LDW and SPAD values, validation using reflectance data indicated better precision to predict LDW and SPAD values, as are represented by their R^2, namely 0.651 and 0.707, respectively.

Meanwhile, the model using SAVI denoted the highest values (R^2 = 0.852), then followed by RDVI (R^2 = 0.845), RVI (R^2 = 0.816) and NDVI (R^2 = 0.785) for predicting LAI.While the validation of predictive model using RVI implied the highest values (R^2 = 0.797), then followed by SAVI (R^2 = 0.756), RDVI (R^2 = 0.754) and NDVI (R^2 = 0.731) for predicting LDW.

Moreover, the test of predictive model using SAVI indicated the highest value (R^2 = 0.658), then followed by RDVI (R^2 = 0.644), RVI (R^2 = 0.566) and NDVI (R^2 = 0.565) for predicting SPAD values. Across entire validation using VIs, RDVI has the best accuracy (R^2 = 0.854) to validate the predictive model of LAI than that of LDW (R^2 = 0.754) or SPAD (R^2 = 0.644). It seems, all VIs have the most significant results in validating predictive model for LAI than that of LDW and SPAD, and beside that, validating predictive model for LDW still points out the significant result (R^2 > 0.731). In general, the accuracy to validate predictive model using VIs as shown in Figure 5 indicates significant value (R^2 > 0.565). Meanwhile, the most significant of R^2 to validate the predictive model is using FDR data with R^2 = 0.859 for LAI.

REFERENCES

Anderson, G.L., and J.D. Hanson (1992), Evaluating hand-held radiometer derived vegetation indices for estimating above ground biomass. Geocarto Int., 1, pp.71-78.

Daughtry, C.S.T., C.L. Walthall, M.S. Kim, E.B. de Colstoum and J.E. Mcmurtrey (2000), Estimating corn leaf chlorophyll concentration from leaf and canopy reflectance. *Remote Sensing of Environment, 74*, 229-239.

Dawson, T.P. and P.J. Curran (1998), A new technique for interpolating the relationship between reflectance red edge position. *International Journal of Remote Sensing, 19*, 2133-2139.

EKO Instruments Co. Ltd. (2004), Portable Spectroradiometer MS-720: *Instruction Manual*. EKO instrument Co Ltd., Tokyo.

Elvidge, C.D. and Z. Chen (1995), Comparison of broad-band and near-infrared vegetation indices. *Remote Sensing of Environment, 54*, 38-48.

Filella, I. and J. Penuelas (1994), The red edge position and shape as indicators of plant chlorophyll content, biomass and hydric status. *International Journal of Remote Sensing, 15*, 1459-1470.

Gilabert, M.A., S. Gandia and J. Melia (1996), Analyses of spectral-biophysical relationships for a corn canopy. *Remote Sensing of Environment, 55*, 11-20.

Huete, A.R (1988), A Soil-adjusted vegetation index (SAVI). *Remote Sensing of Environment, 25*, 295-309.

Kumar, L., K.S. Schmidt, S. Dury and A.K. Skidmore (2001), Imaging spectrometry and vegetation science. In *Imaging Spectrometry*, edited by F. van der Meer and S. M. de Jong, Kluwer Academic.

Lichtenthaler, H.K., A. Gitelson and M. Lang (1996), Non-destructive determination of chlorophyll content of leaves of a green and an aurea mutant tobacco by reflectance measurements. *Journal of Plant Physiology, 148*, 483-493.

Savitzky, A. and E.J.M. Golay (1964), Smoothing and difference of data by simplified least squares procedures. *Analytical Chemistry*, 36, 1627-1639.

Shibayama, M., and T. Akiyama (1991), Estimating grain yield of mature rice canopies using high spectral resolution reflectance measurements. *Remote Sensing of Environment, 36*, 45-53.

Thenkabail, P.S., R.B. Smith and E. De Pauw (2001), Hyperspectral vegetation indidces and their relationships with agricultural crop characteristics. *Remote Sensing of Environment, 71*, 158-182.

Tucker, C.J. (1979), Red and photographic infrared linear combinations for monitoring vegetation. *Remote Sensing of Environment, 8* (1), 127-150.

Tucker, C.J., J.H. Elgin Jr., J.E. McMurtrey III and C.J. Fan (1979), Monitoring corn and soybean crop development with hand-held radiometer spectral data. *Remote Sensing of Environment, 8*, 237-248.

Wanjura, D.F. and J.L. Hatfield (1987), Sensitivity of spectral vegetation indices to crop biomass. *Trans. ASAE, 30*(3), 810-816.

Yang, C.M. and M.R. Su (1997), Seasonal variations of reflectance spectrum and vegetation index in rice vegetation cover.p.574-593. In *Proc. of the 3rd Asian Crop Sci. Conf.*, Taichung, Taiwan.27 April-2 May 1998. Chinese Society of Agronomy, Taichung, Taiwan.